

HOSTED BY



ELSEVIER

Gulf Organisation for Research and Development

International Journal of Sustainable Built Environment

ScienceDirect
www.sciencedirect.com

Original Article/Research

A comparative study on optimum insulation thickness of walls and energy savings in equatorial and tropical climate

Modeste Kameni Nematchoua^{a,*}, Paola Ricciardi^a, Sigrid Reiter^b, Andrianaharison Yvon^c

^a Department of Civil Engineering and Architecture, University of Pavia, Via Ferrata 1, 27100 Pavia, Italy

^b LEMA, Faculty of Applied Sciences, University of Liege, Liege, Belgium

^c Department of Electrical Engineering, National Higher Polytechnical School of Antananarivo, Madagascar

Received 21 November 2016; accepted 17 February 2017

Abstract

The increase outdoor temperature acts directly on the indoor climate of buildings. In Cameroon, the energy consumption demand in the buildings sector has been rapidly increasing in recent years; so well that energy supply does not always satisfy demand. Thermal insulation technology can be one of the leading methods for reducing energy consumption in these new buildings. However, choosing the thickness of the insulation material often causes high insulation costs. In the present study, the optimum insulation thickness, energy saving and payback period were calculated for buildings in Yaoundé and Garoua cities, located in two climatic regions in Cameroon. The economic model including the cost of insulation material and the present value of energy consumption and the cost over a life time of 22 years of the building, were used to find the optimum insulation thickness, energy saving, and payback period. Materials that extruded polystyrene were chosen and used for two typical wall structures (concrete block (HCB) and compressed stabilized earth block wall (CSEB)). The early cooling transmission loads, according to wall orientations and percentage of radiation blocked were calculated using the explicit finite-difference method under steady periodic conditions. As a result, it was found that the west- and east-facing walls are the least favourite in the cooling season, whereas the south and north orientations are the most economical. Although wall orientation had a significant effect on the optimum insulation thickness, it had a more significant effect on energy savings. In equatorial region (Yaoundé), for south orientation, the optimum insulation thickness was 0.08 m for an energy savings of 51.69 \$/m². Meanwhile, in tropical region (Garoua), for north orientation, the optimum insulation thickness was 0.11 m for an energy savings of 97.82 \$/m².

© 2017 The Gulf Organisation for Research and Development. Production and hosting by Elsevier B.V. All rights reserved.

Keywords: Energy savings; Optimum insulation; Equatorial and tropical climate; Buildings; Wall orientation

1. Introduction

One of the most efficient ways to reduce the transmission rate of heat and energy consumption to cool and heat

buildings is the use of an appropriated thermal insulation in the building envelope. An optimum thickness of insulation offers minimum total cost, including the cost of insulation and energy consumption on the building life (Daouas, 2011). In Cameroon, energy consumption in modern and traditional buildings has considerably increased in recent years, and unfortunately, no measure has been taken by the Cameroon government to improve the thermal quality of the building envelope. A comfortable environment is

* Corresponding author.

E-mail address: kameni.modeste@yahoo.fr (M. Kameni Nematchoua).

Peer review under responsibility of The Gulf Organisation for Research and Development.

<http://dx.doi.org/10.1016/j.ijse.2017.02.001>

2212-6090/© 2017 The Gulf Organisation for Research and Development. Production and hosting by Elsevier B.V. All rights reserved.

Nomenclature

As	annual energy savings ($\$/\text{m}^2$)	q_i	heat flux density at indoor surface of the wall (W m^2)
c	specific heat ($\text{J kg}^{-1} \text{K}^{-1}$)	Q_c	annual cooling transmission load (MJ m^{-2})
C	cost (\$)	sd	shade level
COP	coefficient of performance of air-conditioning system	t	time (s)
CDD	degree-days ($^{\circ}\text{C days}$)	T	temperature (C)
g	inflation rate (%)	x	coordinate direction normal to wall (m)
h	combined heat transfer coefficient ($\text{W m}^{-2} \text{K}^{-1}$)	<i>Greek symbols</i>	
H	monthly average of daily global radiation on horizontal surface ($\text{MJ m}^{-2} \text{day}^{-1}$)	α	solar absorptivity of outside surface of wall
H_o	monthly average of daily extraterrestrial radiation on horizontal surface ($\text{MJ m}^{-2} \text{day}^{-1}$)	γ	surface azimuth angle ($^{\circ}$)
H_d	monthly average of daily diffuse radiation on horizontal surface ($\text{MJ m}^{-2} \text{day}^{-1}$)	δ	declination angle ($^{\circ}$)
L	wall thickness (m)	λ	thermal conductivity ($\text{W m}^{-1} \text{K}^{-1}$)
L_{op}	optimum insulation thickness (m)	ϕ	latitude ($^{\circ}$)
I	interest rate (%), order of node	w	hour angle ($^{\circ}$)
I_{total}	solar radiations on the horizontal surface (W m^2)	w_s	sunset-hour angle for a horizontal surface ($^{\circ}$)
I_b	direct solar radiations on the horizontal surface (W m^2)	ρ	density of material (kg m^3)
I_d	diffuse solar radiations on the horizontal surface (W m^2)	ρ_r	ground reflectivity
I_o	hourly extraterrestrial radiation (W m^2)	<i>Subscripts</i>	
N	number of nodes	el	electricity
n	lifetime of building (years)	enr	energy
M	number of layers of composite wall	I	inside
p_b	payback period (years)	ins	insulation
		max	maximum value
		min	minimum value
		o	outside
		sa	solar-air
		t	total

necessary for an individual's health and productivity in a building (Kameni Nematchoua, 2014). A considerable applied insulation thickness on the external walls of the buildings results in significantly lower heat load transmission. The cost of the insulation material increases linearly with the thickness of the insulation material (Ozel, 2011). In 2008, it has been shown that more than 50% of the consumed total energy in the building has been dedicated to heating and cooling (Kameni Nematchoua, 2015). This percentage is going to rise in the coming years, as the global population continues to increase (Kameni Nematchoua, 2015). Thermal insulation is also solicited to reduce the loss of heat in buildings through the envelope.

Meanwhile, the use of the most efficient energy to cool buildings is the best measure to preserve energy and protect environment (Azmi Aktacir et al., 2010; Özden et al., 2011). There are many studies in the literature on the determination of optimum insulation thickness on building walls, and most of them had used the degree day (or degree hour) to calculate the thickness (Ucar and Balo, 2009, 2010; Comakli and Yüksel, 2003; Dombayci et al., 2006; Daouas et al., 2010; Bolattürk, 2008; Yu et al., 2009;

Ghrab-Morcos, 2002). For instance, Bolattürk (Bolattürk, 2006) analysed the use of insulation on the external walls of buildings during many seasons, and found that the building inertia influences indoor comfort. A good selection of construction materials is very important at the time of conception of building. Tsilingiris (Tsilingiris, 2003) developed a numerical algorithm for the cooling load calculation, while Granja and Labaki (2003) presented a periodic solution of the heat flow through a flat roof using Fourier analysis. These results have facilitated the calculation of architects. Furthermore, Dombayci et al. (2006) found the optimum insulation thickness of the external wall for different energy sources and different insulation materials. The study by Mohsen et al. (2001) showed that the insulation of external walls and roofs can increase energy saving by up to 77%. Meanwhile, Naouel Daouas et al. (2010) found that the most profitable case for insulation is the stone/brick sandwich wall and expanded polystyrene, with an optimum thickness of 5.7 cm, which achieved energy savings up to 58% with a payback period of 3.11 years. This work, has allowed to improve the results obtained in Tsilingiris (2003), Granja and Labaki (2003),

Dombayci et al. (2006). Hanan et al. (2011) identified several design-related faults common in Saudi Arabian house design, which contributed to inefficient use of energy. Kemal and Bedri (2003) showed that optimization is based on the lifecycle cost analysis, and obtained an able energy saving by applying optimum insulation thickness. Farshid et al. (2014), showed that the sustainability scenario could offer, approximately, 100% increase in the optimum thickness of extra insulation compared to the Business As Usual scenario (BAU). However, the implication of different life spans of 40, 50 or 60 years, on the optimum measure appeared to be either negligible or very small, depending on the chosen scenario. It must be noted that the results obtained in each of these studies differed according to the study places with their climate zone. In the Sub-Sahara Africa regions, ambient temperatures and solar radiation levels are sufficiently high that, even during winter, buildings do not need energy for heating. The roof insulation is as important as that of wall. This work is the continuation of Wati and Meukam (2015). The choice of Yaounde and Garoua as the main investigation field cities has not been made randomly. Several countries in sub-Saharan Africa and Asia have a climate similar to that of these two cities. In this sense, the results can also serve as a standard for construction and design of buildings in these different regions and also improve Existing ASHRAE database. In addition, Yaoundé and Garoua are two cities with a very high population density in Central Africa. These cities are highly threatened by the effects of climate change, which explains the high energy demand for cooling in new residences.

The aim of the present study was to determine optimum insulation thickness for external walls of buildings in two climate areas of Cameroon. Optimization was based on an economic model, in which a lifecycle cost analysis was conducted using one type of insulation material and two typical wall structures. The yearly cooling transmission loads according to wall orientations were calculated using explicit finite-difference method under steady periodic conditions. In addition, the thermal performance of the walls under optimal conditions was also investigated.

2. Methodology

2.1. Analysed cities

The Yaoundé city is built on several hills and enjoys a picturesque setting and a relatively “fresh” climate. It is the capital of the central region and also the Cameroon political capital. This city is located between 3°52'N and 11°31'E, then, around of 726 m of altitude. Precipitation ranges from 22 mm (January) to 298 mm (October). In February, the average temperature is 24.9 °C. February is therefore the hottest month of the year. August is the coldest month of the year. The average temperature is 22.2 °C during this period. Yaounde city is approximately 300 km from the Atlantic coast and enjoys a temperate

sub-equatorial climate with four seasons, including a long dry season (mid-November to late March), a short rainy season (April to mid-June), a short dry season (mid-June to mid-August) and a long rainy season (mid-August to mid-November). Its population was about 2.5 million in 2011, and since the early 1990 s, the population has increased with a growth rate of 7% per year.

Located between 9°18'N and 13°23'E, around altitude 199 m; Garoua is the capital of the northern region of Cameroon. It has approximately 357,000 inhabitants. Garoua city is the third largest city of Cameroon. In this city, scorching heat can be experienced in the late dry season despite the shade provided by the trees that line the main streets, and the average monthly temperature is 26 °C in August and 40 °C in March (extreme temperatures varied from 17 °C to 46 °C). It has Sudanian-type tropical climate. It is characterized by a long dry season from October to April and a short rainy season from May to September. The total monthly rainfall varies from 0 to 250 mm. Its monthly sunshine varies from 194 to 300 h.

2.2. Mathematical formulation

The walls of the modern houses in the sub-Saharan Africa, in general, and in Cameroon, in particular, are generally made with parpen, with a cement coating on each side. However, the development of techniques for stabilizing mud brick (mechanical and chemical) has led to a renewed interest in it. Thus, to optimize the thickness of the insulation in the walls in modern homes, composite walls are considered (Fig. 1).

The outside face of the wall is subjected to variations in temperature $T_o(t)$ and solar radiation $I(t)$. The inside face of wall comes in contact with the indoor air maintained at a fixed temperature for T_i to have better thermal comfort. Each layer, J , of the composite wall is therefore the seat of a unidirectional transfer of heat in the supposed case was defined as in (Kameni Nematchoua, 2015).

$$\rho_j c_j \frac{\partial T_j}{\partial t} = \lambda_j \frac{\partial^2 T_j}{\partial x^2} \quad (1)$$

where j refers to the serial number of the layer ($j = 1, \dots, M$ for a wall of M layer); x and t are the spatial and temporal coordinates, respectively; T_j is the temperature at the point of coordinates x in layer j and ρ_j , c_j and λ_j are the density, specific heat and thermal conductivity of the material of layer j , respectively. The resolution of Eq. (1) requires the determination of the boundary conditions and initial condition. Thus, at the initial moment, we assume that all points of the wall have the same temperature (25 °C). The outside face conditions and indoor condition are given by Eqs. (2) and (3), (see Daouas, 2011), respectively.

$$-\lambda_1 \left(\frac{\partial T}{\partial x} \right)_{x_1=0} = h_o(T_o - T_1) + \alpha I \quad (2)$$

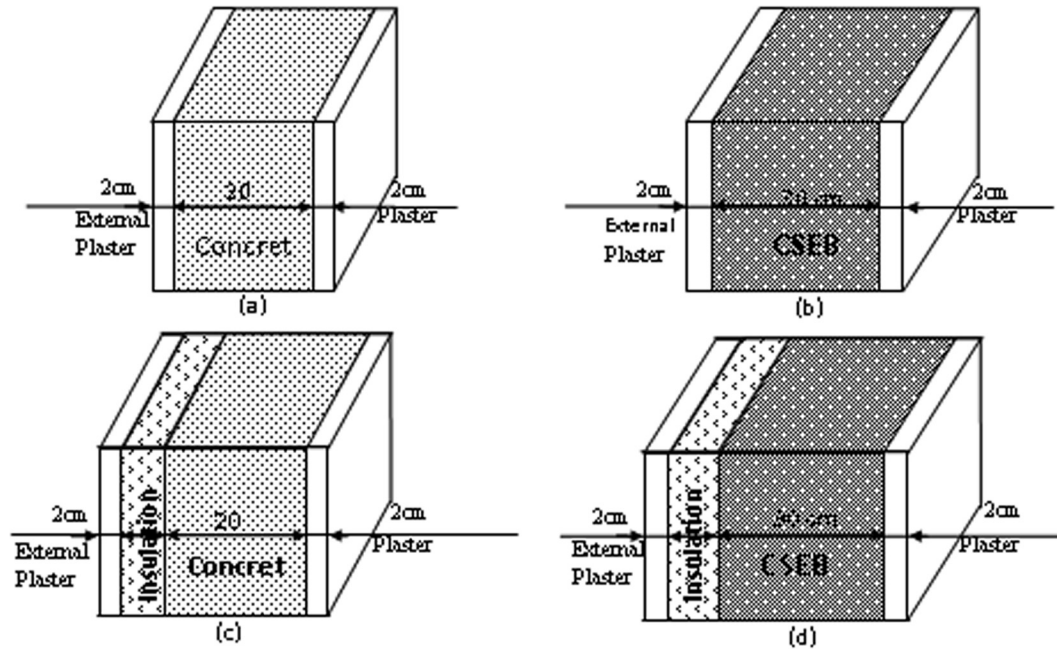


Fig. 1. Typical wall structures (a: hollow concrete block wall, b: CSEB wall) and proposed wall structures (c: insulated hollow concrete block wall, d: insulated CSEB wall).

$$-\lambda_M \left(\frac{\partial T}{\partial x} \right)_{x=L} = h_i(T_N - T_i) \quad (3)$$

where α is the absorption coefficient and h_e and h_i are the thermal exchange coefficient on the outside and inside faces, respectively. Their values ($h_e = 22W.m^{-2}.K^{-1}$ and $h_i = 9W.m^{-2}.K^{-1}$) were obtained from a previous study (Ozel, 2011). I is the radiation of short wavelength received by outdoor face wall (vertical), and was obtained using Eq. (4) given in Ozel (2011).

$$I = I_d R_b + \frac{1}{2} \rho_y I_h + \frac{1}{2} D_h \quad (4)$$

where I_d, D_h and I_h are the direct radiation, diffuse radiation and global radiation on a horizontal surface, respectively and ρ_y is the albedo of the area assumed to be equal to 0.2. The parameter R_b is given for a vertical surface by Ozel (2011).

$$R_b = \frac{\cos \delta \sin \phi \cos \omega + \cos \delta \sin \gamma \sin \omega - \sin \delta \cos \phi \cos \gamma}{\cos \phi \cos \delta \cos \omega + \sin \phi \sin \delta} \quad (5)$$

where δ, ω, γ and ϕ are the solar declination, hourly angle, surface of the azimuth and solar elevation, respectively. γ is equal to 0 for an inclined surface facing south, -90 for a surface turned towards east, 90 for a surface turned towards west and 180 for a north surface.

The third term of Eq. (4) designating the diffuse radiance on a vertical surface was obtained from a model developed in El-Sebaï et al. (2010). This model uses the simplifying hypothesis of a distribution isotrope of the diffuse radiation that is independent of the zénithal and azimuthal angles.

2.3. Method of solution

To solve the above-mentioned problem, a thermal model of an area consisting of a wall was constructed from the component library of Ham-tools developed in the environment of MATLAB-Simulink simulation (Kolaitis et al., 2013). The Ham-tools has been developed jointly by Chalmers University of Technology (Sweden) and the University of Technology in Denmark (Copenhagen, Denmark), and is solved numerically using the finite-difference method and a scheme of explicit temporal resolution (Eq. (1)). For a stitch of thickness d_i inside the materials (Fig. 2), the thermal balance at node i mesh centre can be written as follows:

$$\frac{T_i^{n+1} - T_i^n}{\Delta t} = \frac{1}{\rho_i c_i d_i} \left(\frac{T_{i-1}^n - T_i^n}{R_{i-1} + R_i} + \frac{T_{i+1}^n - T_i^n}{R_{i+1} + R_i} \right) \quad (6)$$

where i denotes the number of node and n indicates the time step. The resistances are defined as (Ozel, 2011):

$$R_i = \frac{d_i}{2\lambda_i} \quad (7)$$

where λ_i is the thermal conductivity of the node material i . As the studied wall is composite, a node is placed at every interface between the two materials of different nature. The complete modelling of the heat transfer to the node of contact is given in Nielsen (2002).

The thermal balances are given by Eqs. (8) and (9), respectively.

$$\frac{T_1^{n+1} - T_1^n}{\Delta t} = \frac{1}{\rho_1 c_1 d_{out}} \left(\frac{T_2^n - T_1^n}{R_2 + R_1} + h_o(T_o - T_1) + \alpha I \right) \quad (8)$$

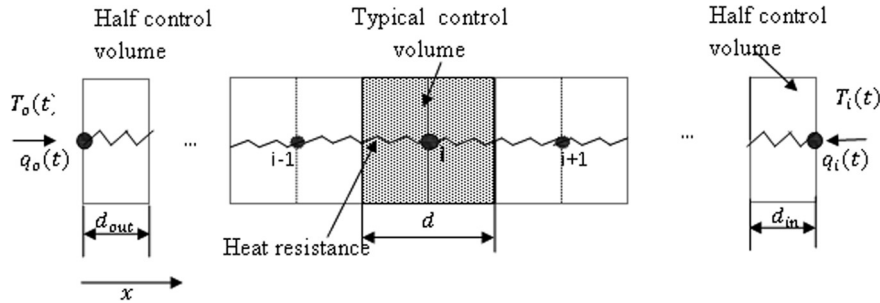


Fig. 2. Numeric model.

$$\frac{T_N^{n+1} - T_N^n}{\Delta t} = \frac{1}{\rho_i c_i d_{in}} \left(\frac{T_{N-1}^n - T_N^n}{R_{N-1} + R_N} + h_i (T_i - T_N) \right) \quad (9)$$

The numeric solution gives the temporal evolution of the temperature to every internal node of the wall and on internal and external face of the wall. The density of heat flux transmitted to the zone is given by El-Sebaï et al. (2010).

$$q_c(t) = \begin{cases} h_i (T_i - T_N(t)) & \text{if } T_i > T_N \\ 0 & \text{if } T_i \leq T_N \end{cases} \quad (10)$$

The maximum step size of the time adopted in our model is an hour, and the hourly exterior conditions are considered.

2.4. Hourly exterior conditions

The monthly averages of the minimum and daily maxima of temperature of every month on a relatively long period (1984–2005) were first calculated from the archives of the Department of Meteorology (Directorate of National Meteorology). These values were used to estimate the middle hourly values of temperature of every month from the model of cosine (Safaeq and Fares, 2011), as shown in Eq. (11).

$$T_t = \frac{T_{max} - T_{min}}{2} \cos\left(\frac{\pi(t-a)}{12}\right) + \frac{T_{max} + T_{min}}{2} \quad (11)$$

where T_t is the temperature at time $t(h)$ starting from midnight (in the range of 1–24); T_{max} and T_{min} are the minimum and maximum daily temperature, respectively and a is the hour of the day at which temperature is maximum. In the present study, the parameter a was considered as 14, as reported by Safaeq and Fares (2011), De Wit (1978).

The daily averages of the diffuse and global radiances on a horizontal surface of every month were obtained by dividing the number of day of the month considered, and the monthly averages of one relatively long period (1985–2005) was obtained from Sola (2014). The hourly averages of the diffuse and global radiances were obtained from the model of decomposition of Lui and Jordan and Collares-Pereira (Basunia et al., 2012), considering the 15th day of the month as the representative day. Figs. 3 and 4 show

the monthly diurnal averages of temperatures and solar radiation levels in Garoua and Yaoundé, respectively.

The outdoor temperature varied from 17.6 °C to 40.9 °C with a standard deviation (SD) of 0.97. A peak was obtained in March at around 2 pm. This peak persisted till April and then fell by 3.9 °C in May. From May, a light reduction in the air temperature was observed until the month of November when the temperature appeared to increase. The global radiation was about 1000 W/m² from January to March, and the direct normal radiation increased up to 825 W/m² in January, while the diffuse radiation was around 300 W/m², except for the period from November to January (Fig. 3). In the equatorial zone (Yaounde), the climatic conditions were more favourable; the outdoor air temperature varied from 21.5 °C to 31.7 °C (SD = 0.74), and the horizontal global radiation was rarely 800 W/m² (Fig. 4). Generally, the global radiation was more important in tropical region than equatorial region. But, almost equal in January and February in the two regions. These different studied elements testified the unequal variation in the energies used for the cooling of the buildings in these regions. The climatic conditions of these cities were often very unfavourable to compare with those of the city of Jeddahen (Hanan et al., 2011).

3. Thermal performance of the uninsulated wall

Hence forth, the composite walls presented in Fig. 1a and b will be designated as wall 1 and wall 2, whose outside faces were exposed to the climatic conditions of the cities of Yaounde and Garoua, respectively. The solar radiation calculations were made for the 15th day of the hottest month of each of the two climates as indicated by Jeddahen (Hanan et al., 2011); i.e., March for Garoua and January for Yaounde. The month of January was chosen for Yaoundé, because of the importance of the amplitude of the diurnal temperature variations. The thermophysical properties of the materials used are given in Table 1.

3.1. Effect of wall orientation

Fig. 5, shows the remarkable effect of wall orientation on the heat flux density on the internal face of every wall model. The peak density of the flux on the internal surface

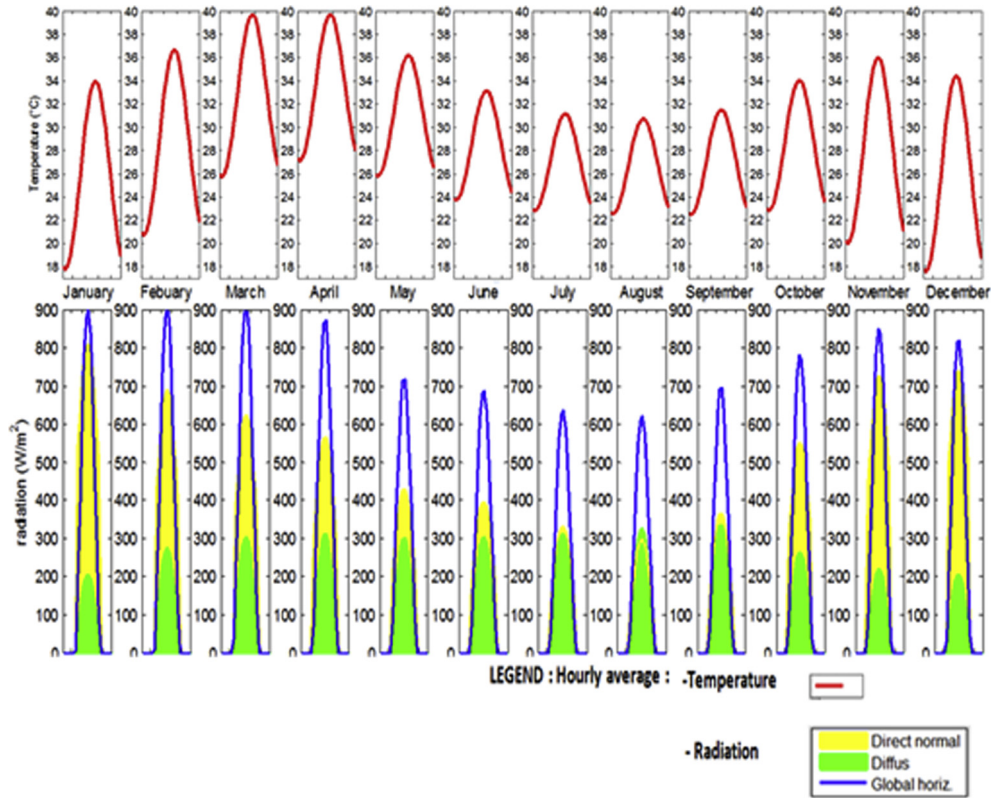


Fig. 3. Monthly diurnal averages of temperatures and solar radiation levels in Garoua.

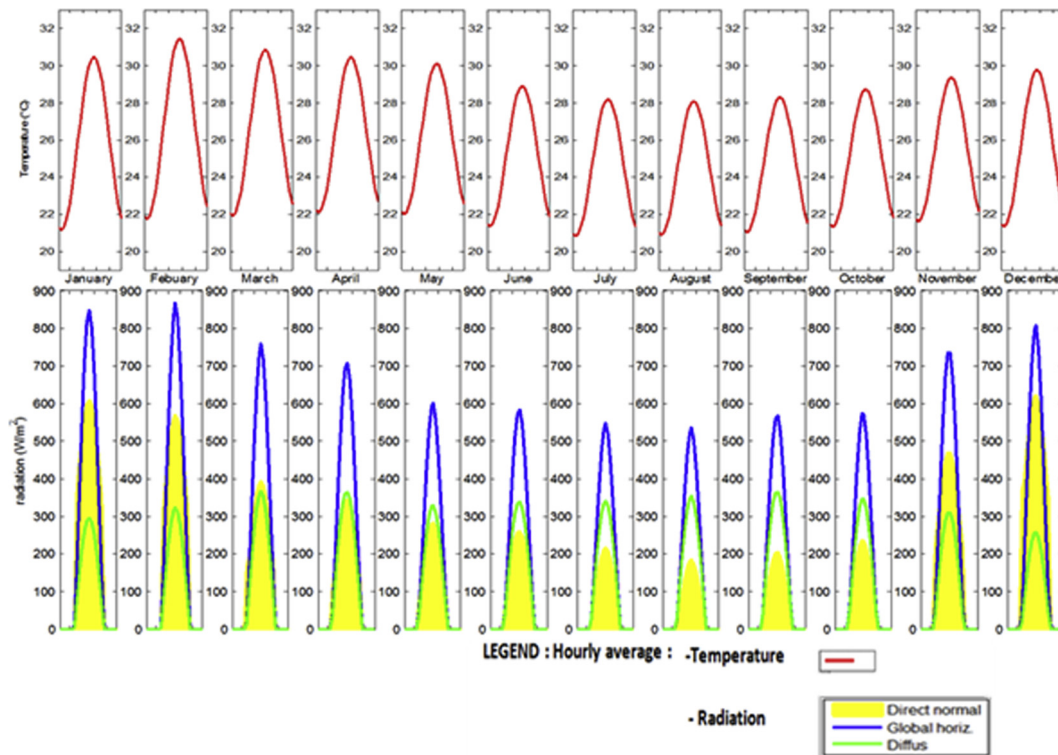


Fig. 4. Monthly diurnal averages of temperatures and solar radiation levels in Yaoundé.

Table 1
Material properties (Meukam et al., 2004; Sisman et al., 2007).

Materials	$\rho(\text{kg}/\text{m}^3)$	$c(\text{J}/\text{kg}/\text{K})$	$\lambda(\text{W}/\text{m}/\text{K})$
Expanded polystyrene	10	1400	0.04
Cement plaster	2200	1050	0.87
Hollow concrete block	1250	880	0.67
CSEB wall	1758	1000	0.887

of walls (1) and (2) was higher when they were oriented towards east in the tropical climate (Garoua) during the representative day of the month of March (Fig. 5a and b). This is due to the fact that this facing is the one that receives more radiance of short wavelength when the outside temperature reaches its maximal value (around 14 h). These heat fluxes of the density peaks on the interior wall faces were observed at around 20 h in the case of wall 1 and at about 24 h in the case of wall 2. The thermal inertia difference between the two types of walls could be the origin of this shift. Indeed, in March, initially, the heat flux density was $30 \text{ W}/\text{m}^2$, it has decreased up to $5 \text{ W}/\text{m}^2$ around of 10 h, then begin to increase till 20 h, where it reaches $40 \text{ W}/\text{m}^2$. In January, at the same time, the heat flux density was near to $25 \text{ W}/\text{m}^2$ (South facing).

During the representative day of the month of January, in Yaoundé, the peak density of heat flux on the internal

face of each type of wall was observed when the wall was oriented southwards (Fig. 5c and d). This is due to the fact that south face receives more solar energy than east, west and north faces at that moment or when the outdoor temperature exhibits maximum variation. As stated previously, the difference between the hours when peaks appear and their values are due to the thermal inertia difference between the two types of walls. In the equatorial region (yaounde), the heat flow density flux was less important than tropical region (Garoua). In March (Yaoundé), at first time, the heat flux density was $25 \text{ W}/\text{m}^2$, then, it has decreased up to $15 \text{ W}/\text{m}^2$, around of 13 h, till 23 h, then it increased and reaches $25 \text{ W}/\text{m}^2$. In January it increased linearly. However, the heat flow density flux on the interior layer of the wall when it was oriented towards north was weaker than that noted when it was oriented towards other directions (south, east and/or west). This could be due to the fact that the north wall received very little solar energy during the representative days of the months considered in the two climates (Fig. 5). The wall orientation influences the heat flux density on its internal face. However, Fig. 5 shows that for the compressed stabilized earth brick (CSEB) (wall 2), fluctuations within the surface conditions were significantly reduced, when compared with those shown by the concrete block wall (wall 1). This is due to the good capacity of the earth bricks to store heat,

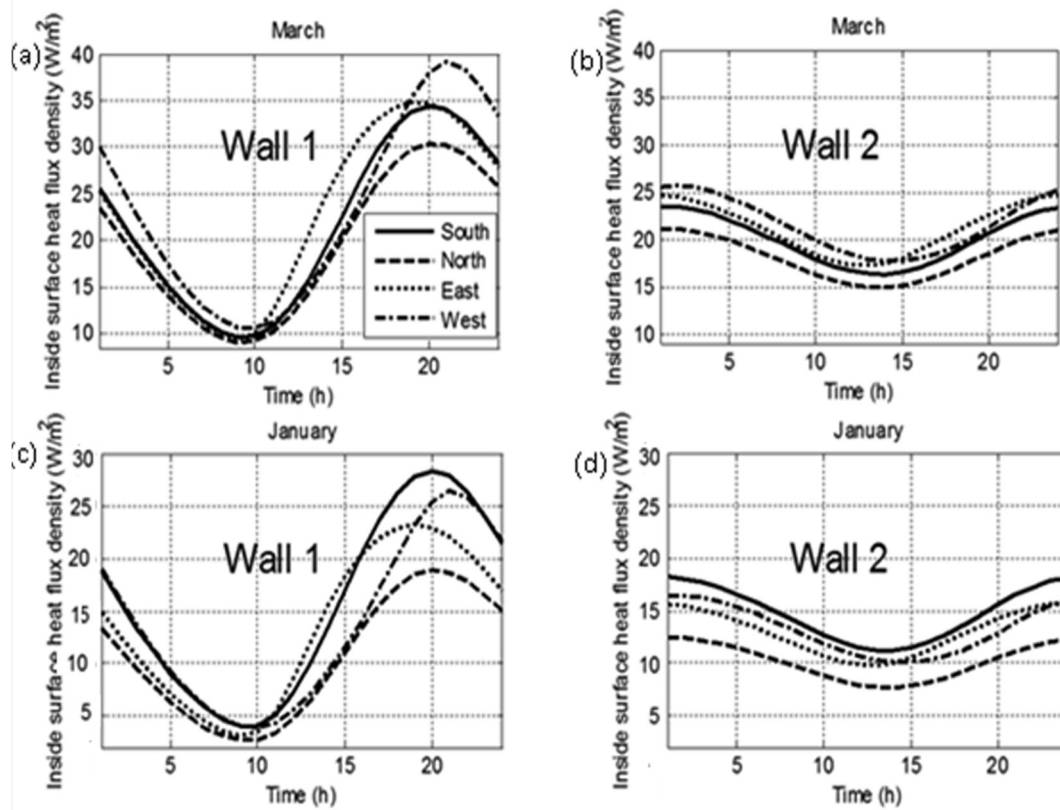


Fig. 5. Effect of wall orientation on the hourly variation of the inside surface heat flux density in Garoua [(a) and (b)] and Yaoundé [(c) and (d)] for the two wall structures.

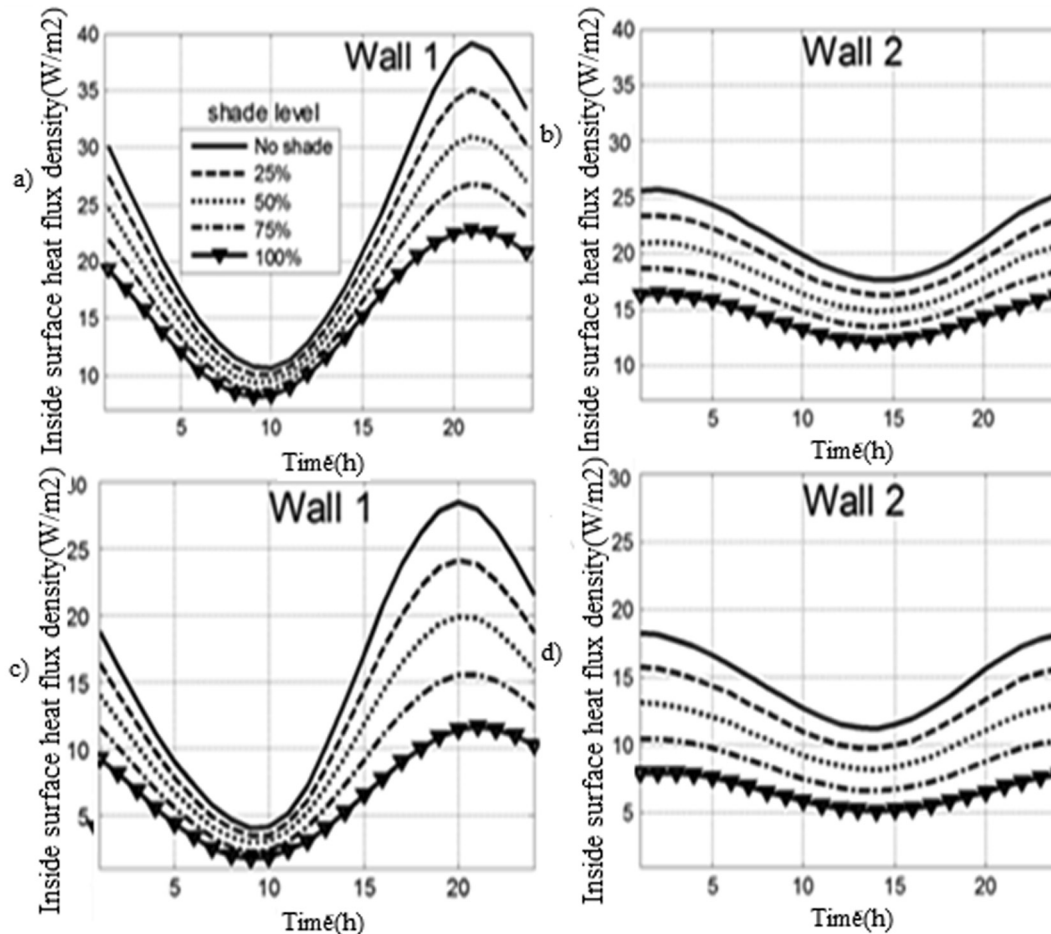


Fig. 6. Effect of solar shading on the inside surface heat flux in Garoua [(a) and (b)] and Yaoundé [(c) and (d)].

when compared with that of the concrete block. These results showed that CSEB, similar to stone wall (Daouas et al., 2010), improves the indoor climate.

3.2. Effect of shading

Fig. 6, shows the shade effect on the heat flux density on the internal layer of wall 1 and wall 2. This effect was noted for the orientations of the wall where the heat flux density on the internal layer presented the most elevated peaks either on the “East face” in Garoua or “South face” in Yaounde. In the case of wall 1, there was a strong reduction in the peaks, whereas wall 2 showed a practically uniform reduction during 24 h. It seen that the heat flux density decreases with increasing shade level. Under the same climatic conditions and same orientation, the heat flux density on the inside of wall 1 and wall 2 was different (Figs. 5 and 6). Meanwhile, the daily thermal gains through these two types of walls, obtained by integrating those measured for 24 h as the function given in Eq. (9), were very close. Thus, at the time of determination of the optimum insulation thickness, only wall 1 was used and these results were valid for wall 2.

4. Optimum insulation thickness

The insulated wall reduces yearly transmission load, which is the main input parameter of any optimum insulation thickness model.

4.1. Yearly cooling load calculation

The cooling period in the climatic zones under field spread throughout the year or nearly the yearly quantity of energy Q_c received by indoor wall was determined by integrating the values obtained for 1 year as the function $q_c(t)$ given by Eq. (9). Fig. 7 shows the variation in the yearly cooling load with insulation thickness in Yaoundé and Garoua. In the two climates, the thermal gains through the east and west faces were practically equal and higher than those of the south or north faces. The thermal gains through the south face were higher than those through the north face because the zones of survey were in the northern hemisphere, where the northward-oriented walls received less solar energy than the southward-oriented ones. Nevertheless, irrespective of the orientation of the wall, the yearly thermal gains decreased with the thickness

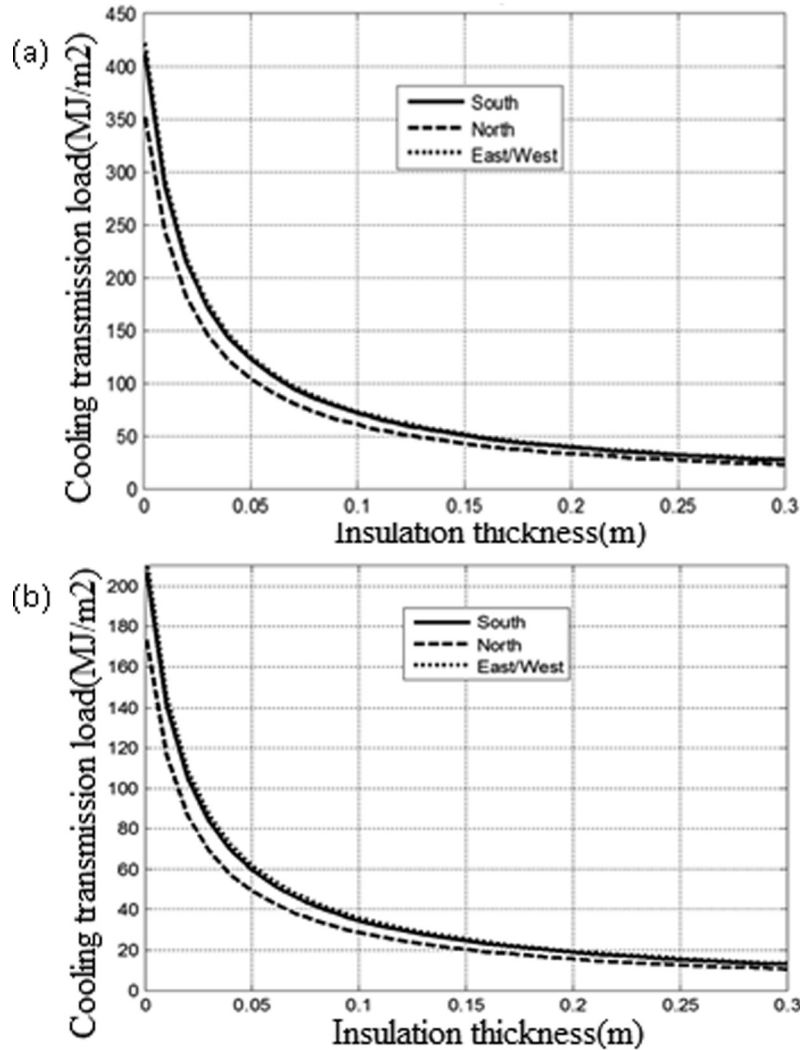


Fig. 7. Cooling transmission load vs. insulation thickness for the climate of Garoua (a) and Yaoundé (b).

of the insulator. These results are similar to those found in the literature (Daouas, 2011; Kameni Nematchoua, 2014; Ozel, 2011; Azmi Aktacir et al., 2010). On the whole, the yearly thermal gains were found to be more important for the climate of Garoua than for the climate of Yaoundé, because the heat degree is more important in Garoua than in Yaoundé (Kemajou, 2011).

Fig. 8a and b shows the influence of the obstruction of radiations of short wavelengths on the yearly thermal gains through east or west face in the two considered climatic zones. This effect was particularly remarkable when the thickness of the insulator was weak. In general, the yearly thermal gains decreased with the percentage of radiation blocked. The last result is similar to those obtained in the literature (Ozel, 2013).

4.2. Economic analysis

The installation of the insulator contributes to the reduction in the air-conditioning load and thus reduction

in the electricity invoice. This reduction is especially important when the thickness of the insulator is large. However, to install an insulator, an initial investment is required, which increases with the thickness of the insulator. The total expense bound to the wall considered during the life-cycle of a building is a function of the thickness of the thermal insulator installed, price of kilowatt-hour of the electric energy, interest rates and inflation of the currency considered. It is important to determine the insulator thickness that minimizes this total amount (C_t), which is equal to the sum of the present cost of the energy consumed during the time of existence of the building and the insulation cost (Daouas et al., 2010).

$$C_t = C_{enr}PWF + C_i = C_{enr}PWF + C_{ins}L_{ins} \quad (12)$$

where C_{enr} ($\$/m^2\text{year}$) is the yearly cost of the electric energy consumed bound to the thermal gains through one square metre of wall; PWF is the “present worth facto”; C_i ($\$/m^3$) is the cost of one cubic metre of insulator and L_i (m) is the insulation thickness.

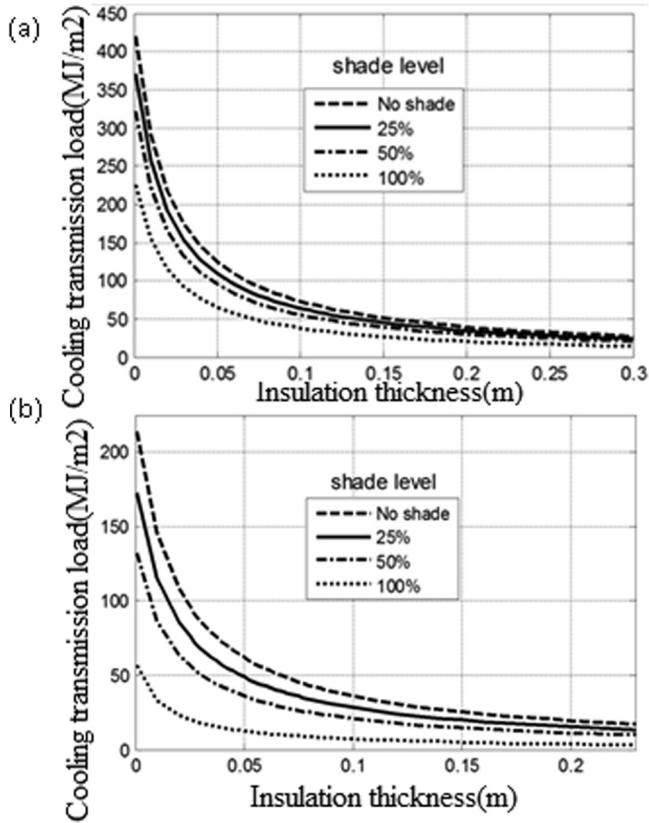


Fig. 8. Effect of solar radiation blocked on yearly cooling load in Garoua (a) and Yaoundé (b).

C_{enr} depends on the yearly thermal gains through the unit wall surface (Q_c), the price of energy kilowatt-hour (C_{el}) and the coefficient of performance of the air-conditioning unit, as given in Eq. (13).

$$C_{enr} = \frac{Q_c C_{el}}{COP} \quad (13)$$

PFW is a function of the interest rates and inflation, and is expressed as (Daouas et al., 2010).

$$PFW = \sum_{u=1}^n \left(\frac{1+i}{1+d} \right)^u = \frac{1+i}{d-i} \left[1 - \left(\frac{1+i}{1+d} \right)^n \right] \text{ if } i \neq d \quad (14)$$

$$PFW = \frac{n}{1+i} \text{ if } i = g \quad (15)$$

where n is the yearly lifecycle of the building, i is the currency inflation rate and d is the interest rate. The pay-back period b is calculated by solving the following equation for b :

$$\frac{C_i}{A_s} = PWF(b) \quad (16)$$

where C_i/A_s is the simple pay-back period that does not take interest rate into account and A_s is the amount of the annual savings obtained by insulation.

The energy savings ($\$/m^2$) obtained during the lifetime of the insulation material can be calculated as (Kameni Nematchoua, 2015):

$$ES = C_{to} - C_{tins} \quad (17)$$

where C_{to} and C_{tins} are the total cost of cooling without and with insulation, respectively. The energy saving can be expressed as% by the following equation (Kameni Nematchoua, 2015):

$$\frac{ES}{C_{to}} 100 = \left(1 - \frac{C_{tins}}{C_{to}} \right) 100 \quad (18)$$

The results obtained from the above-mentioned method can be compared with those of the degree-day method. In fact, the degree-day method has been used by several authors to estimate the optimal insulation thickness. In this method, the yearly transmission load per unit of wall area is estimated (in J/m^2) by the following equation (Kameni Nematchoua, 2015):

$$Q_c = 86400 \cdot U \cdot CDD \quad (19)$$

where CDD is the annual cooling degree-day (in °C days) whose values for the climate of Garoua and Yaoundé are 1315 and 361, respectively. These values are calculated from the meteorological data (from Directorate of National Meteorology) for a long period (20 years). The annual cooling degree-day can be obtained by the summation of the positive difference between the mean daily temperature and the fixed indoor base temperature (25 °C) over the whole year. The mean daily temperature can be calculated by adding the maximum and minimum temperatures for the day, and then dividing it by 2 (ASHRAE (2009).

The overall heat transfer coefficient of the wall can be expressed by Eq. (20).

$$U = \frac{1}{R_o + R_{ins} + R_w + R_i} \quad (20)$$

where R_o and R_i are the heat resistance due to convective transfer on the outside and inside surface of the wall, respectively and R_{ins} and R_w are the heat resistance of the insulation layer and rest of the wall, respectively.

The total cost (cost of energy and insulation) is given as (Kameni Nematchoua, 2015):

$$C_t = \frac{0.024 CDD}{COP} \left(\frac{1}{R_t + \frac{L_{ins}}{\lambda_{ins}}} \right) C_{el} PWF + C_{ins} L_{ins} \quad (21)$$

Table 2

The parameters used in the calculations (Sisman et al., 2007; Ghrab-Morcos, 2002).

Parameters	Values
Electricity for cooling Cost ($\$/kWh$)	0.1583
COP	2.5
Expanded polystyrene Cost ($\$/m^3$)	164.32
Inflation rate, i	2.9%
Interest rate, d	5%
Life time, n	30

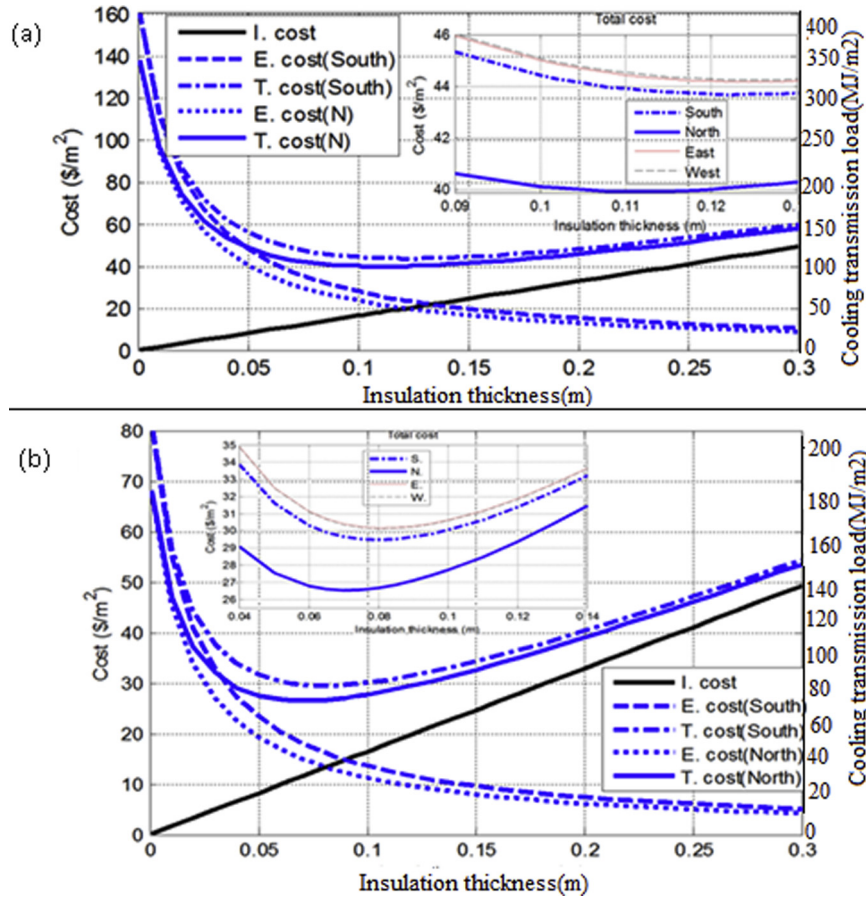


Fig. 9. Insulation cost, energy cost and total cost vs. insulation thickness for different wall orientations in Garoua (a) and Yaoundé (b).

Table 3

The optimum insulation thickness, energy savings and payback period for all wall orientations for Yaoundé and Garoua climate.

Locality	Yaoundé				Garoua			
	South	North	East/West	CDD	South	North	East/West	CDD
Optimum insulation thickness (m)	0.08	0.07	0.08	0.034	0.12	0.11	0.125	0.0835
Energy savings (%)	79.87	77.89	79.71	62.24	85.31	84.36	85.65	80.21
Payback period (years)	4.78	5.14	4.63	9.31	3.39	3.69	3.38	4.66

where L_{ins} and λ_{ins} are the thickness and thermal conductivity of the insulating material, respectively.

$$R_t = R_o + R_w + R_i \tag{22}$$

The optimal insulation L_{op} is the thickness of the insulation layer that corresponds to that minimizing the total cost (Kameni Nematchoua, 2015).

$$L_{op} = \left(0.024 \frac{CDD \lambda_{ins} C_{el} PWF}{C_{ins} COP} \right)^{1/2} - \lambda_{ins} R_t \tag{23}$$

The parameters used in the calculation of the optimum insulating thickness are given in Table 2.

5. Results and discussion

The optimum insulation thickness is calculated by considering the sequential reduction in the cost of the

consumed energy. However, purchase and installation of the insulation layer increase the initial cost of construction. Therefore, an economic analysis was performed in the present study to estimate the optimum insulation thickness, which minimizes the total cost, including the insulation and energy consumption costs.

Fig. 9 shows the insulation cost, energy cost and total cost vs. insulation thickness for different wall orientations. When the energy cost decreases with the increasing insulation thickness, the insulation cost increases linearly with the insulation thickness. This can be explained by the fact that when the insulator transverse measurements are stationary, the cost is proportional to its thickness. The variations in the costs of the electric energy according to the insulator thickness have the pace of those of the thermal gains. Indeed, in the adopted economic model, these quantities are proportional. The total cost is the sum of

the insulation and energy cost. The total cost function of the insulator thickness has a minimum value. The insulator thickness corresponding to this value constitutes the optimal thickness sought. The most economical case with respect to the minimum total cost is the south orientation followed by north, then, east and west orientations. This result is in conformity with those presented in the literature (Kameni Nematchoua, 2015; Farshid et al., 2014). Nevertheless, the minimum total cost can vary according to the type of climate associated with the studied region. In tropical zone (Fig. 9a), the least economical case is the west/east orientation. In equatorial zone (Fig. 9b), the least economical case is the east orientation followed by the west. These results are in agreement with those reported by Naouel Daouas (Daouas, 2011).

Table 3 shows the insulator optimal thickness, the payback period on investment and energy savings according to the different orientations of the wall and climates of the two cities examined. The table also presents a comparison between the results obtained in the present study and those of the degree-day model (DD). In Yaoundé, the optimum insulation thickness is 0.07 m for North orientation. It corresponds to an annual energy saving of 77.89% for 5.14 years, as payback period. However, for the same climate, the insulation optimum thickness is 0.08 m for the East/West orientation. It corresponds to an annual energy saving of 79.71% for 4.63 years, as payback period. On the other hand, in Garoua, the insulation optimum thickness is 0.11 m for the North orientation. It corresponds to an annual energy saving of 84.36% for 3.69 years, as payback period. However, the optimum insulation thickness is 0.125 m for the East/West orientation, for an annual energy saving of 85.65%. An analysis of these results shows that optimum insulation thickness is higher in the tropical climate (Garoua) than in the equatorial climate (Yaoundé), however, the payback period is the weakest in Garoua.

Fig. 10 shows the variation in the energy savings vs. insulation thickness for all wall orientations. The energy savings was maximum for an insulator thickness equal to its optimal value. Beyond this value, an increase in the insulator thickness resulted in a decrease in energy savings. It can be noted from these figures that the lowest value of energy savings was obtained for north and south walls, while the highest energy savings were obtained for the East/West walls. These findings are similar to those obtained by Ozel (2011). For every wall orientation, the insulator optimal thickness decreased with the percentage of radiation blocked.

Indeed, as shown previously, the percentage of radiations blocked increased with the decrease in the yearly thermal gains and thus the insulator optimal thickness. With 100% radiations blocked and in every climate, the insulator optimal thickness remained the same for all wall orientations and was appreciably equal to the one obtained with the “Cooling Degree Day model”. The “Cooling Degree Day model” does not consider the solar radiations in the assessment of CDD.

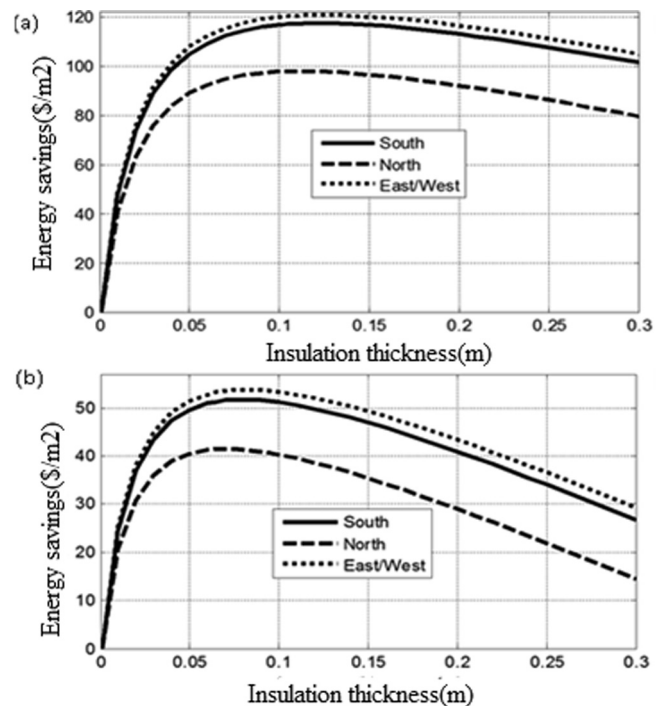


Fig. 10. Variation in energy savings vs. insulation thickness for all wall orientations in Garoua (a) and Yaoundé (b).

6. Conclusion

In the present study, a model was built using MATLAB/Simulink with the help of IBPT (International Building Physics Toolbox) library to determine a numerical solution of transient heat transfer through multilayer walls submitted to the average outdoor temperature and solar radiation specific to the climate of Garoua and Yaoundé. With this method, the inside surface heat flux of two common uninsulated walls (concrete block and CSEB) was predicted. The results presented for the representative day of the hottest month of the considered climate showed the significant effect of wall orientation and solar shading on the thermal performance of the two walls. The yearly cooling transmission load vs. insulation thickness showed a significant effect of wall orientation. The east and west orientations were the least favourable in the considered climate, whereas the north orientation was more favourable. Solar shading significantly reduced the yearly cooling transmission load. In the Yaoundé climate, south orientation was the most economic one with an optimum insulation thickness of 8 cm, 79.87% of energy saving and a payback period of 4.78 years, whereas in the Garoua climate, the east/west orientation was the most economic one with the optimum insulation thickness of 12.5 cm, 85.65% of energy saving and 3.38 years of payback period. The optimum insulation thickness decreased linearly with the percentage of blocked solar radiation. The values obtained with 100% blocked solar radiation were similar to those obtained with the degree-day model. The energy saving was maximum for an insulator thickness equal to its optimal value. Beyond

this value, an increase in the insulator thickness resulted in a decrease in energy savings. The procedure proposed in this work should allow other investigations where different climatic conditions can be considered to reduce energy consumption demand in the buildings. The next work will have as purpose of study the case of roof insulation in these regions and their orientation.

Acknowledgements

The authors of this article acknowledge the Centre for International Cooperation and Development (CICOPS) Project for their support in this work.

References

- ASHRAE, 2009. Handbook-Fundamentals. American Society of Heating, Refrigerating and Air-conditioning Engineers, Inc..
- Azmi Aktacir, Mehmet, Büyükalaca, Orhan, Yilmaz, Tuncay, 2010. A case study for influence of building thermal insulation on cooling load and air-conditioning system in the hot and humid regions. *Appl. Energy* 87, 599–607.
- Basunia, M., Yoshio, H., Abec, T., 2012. Simulation of solar radiation incident on horizontal and inclined surfaces. *TJER* 9 (2), 27–35.
- Bolattürk, A., 2006. Determination of optimum insulation thickness for building walls with respect to various fuels and climate zones in Turkey. *Appl. Therm. Eng.* 26, 1301–1309.
- Bolattürk, A., 2008. Optimum insulation thickness for building walls with respect to cooling and heating degree-hours in the warmest zone of Turkey. *Build. Environ.* 43, 1055–1064.
- Comakli, K., Yüksel, B., 2003. Optimum insulation thickness of external walls for energy savings. *Appl. Therm. Eng.* 23, 473–479.
- Daouas, Naouel, 2011. A study on optimum insulation thickness in walls and energy savings in Tunisian buildings based on analytical calculation of cooling and heating transmission loads. *Appl. Energy* 88, 156–164.
- Daouas, N., Hassen, Z., Ben, Aissia H., 2010. Analytical periodic solution for the study of thermal performance and optimum insulation thickness of building walls in Tunisia. *Appl. Therm. Eng.* 30, 319–326.
- De Wit, C.T., 1978. Simulation of assimilation, respiration and transpiration of crops. *Pudoc, Wageningen*, p. 148.
- Dombayci, Ö.A., Gölcü, M., Pancar, Y., 2006. Optimization of insulation thickness for external walls for different energy-sources. *Appl. Energy* 83, 921–928.
- Dombayci, Ö.A., Gölcü, M., Pancar, Y., 2006. Optimization of insulation thickness for external walls using different energy-sources. *Appl. Energy* 83 (9), 921–928.
- El-Sebaei, A.A., Al-Hazmi, F.S., Al-Ghamdi, A.A., Yaghmour, S.J., 2010. Global, direct and diffuse solar radiation on horizontal and tilted surfaces in Jeddah, Saudi Arabia. *Appl. Energy* 87, 568–576.
- Farshid, B., Dodoo, A., Gustavsson, L., 2014. Cost-optimum analysis of building fabric renovation in a Swedish multi-story residential building. *Energy Build.* 84, 662–673.
- Ghrab-Morcos, 2002. Institut de l'énergie et de l'environnement de la Francophonie. Efficacité énergétique de la climatisation des bâtiments en région tropicale, 1–170, Tome 1.
- Granja, A.D., Labaki, L.C., 2003. Influence of external surface color on the periodic heat flow through a flat solid roof with variable thermal resistance. *Int. J. Energy Res.* 27, 771–779.
- Taleb, Hanan M., Sharples, Steve, 2011. Developing sustainable residential buildings in Saudi Arabia: a case study. *Appl. Energy* 88, 383–391.
- Kemajou, A., et Mba, L., 2011. Matériaux de construction et confort thermique en zone chaude Application au cas des régions climatiques camerounaises. *Revue des Energies Renouvelables* 14, 239–248, N°2.
- omakli, Kemal C., Bedri, Y., 2003. Optimum insulation thickness of external walls for energy saving. *Appl. Therm. Eng.* 23, 473–479.
- Kolaitis, D.I., Malliotakis, E., Kontogeorgos, D.A., Mandilaras, I., Katsourinis, D.I., Founti, M.A., 2013. Comparative assessment of internal and external thermal insulation systems for energy efficient retrofitting of residential buildings. *Energy Build.* 64, 123–131.
- Meukam, P., Jannot, Y., Noumowe, A., Kofane, T.C., 2004. Thermo physical characteristics of economical building materials. *Constr. Build. Mater.* 18, 437–443.
- Kameni Nematchoua, Modeste, Tchinda, René, Djongyang, Noël, Ricciardi, Paola, 2014. A field study on thermal comfort in naturally-ventilated buildings located in the equatorial climatic region of Cameroon. *Renewable Sustainable Energy Rev.* 39, 381–393.
- Kameni Nematchoua, Modeste, Raminosoa, Chrysostôme R.R., Mami-harijaona, Ramarason, René, Tchinda, Orosa, José A., Elvis, Watis, Meukam, Pierre, 2015. Study of the economical and optimum thermal insulation thickness for buildings in a wet and hot tropical climate: case of Cameroon. *Renew. Sustain. Energy Rev.* 50, 1192–1202.
- Mohsen, M.S., Akash, B.A., 2001. Some prospect of energy savings in buildings. *Energy Convers. Manage.* 42, 1307–1315.
- Nielsen, T.R., Peuhkuri, R., Weitzmann, P., Gudum, C., 2002. Modeling Building Physics in Simulink, 2–15 <http://www.ibpt.org> (Accessed 29 September 2014).
- Özden, A., Özgür, A., Hakan, D., İsmail, T., 2011. Environmental impact of optimum insulation thickness in buildings. In: *World Renewable Energy Congress, Sweden*, 8–13.
- Ozel, Meral., 2011. Effect of wall orientation on the optimum insulation thickness by using a dynamic method. *Appl. Energy* 1 (7).
- Ozel, M., 2013. Determination of optimum insulation thickness based on cooling transmission load for building walls in a hot climate. *Energy Convers. Manage.* 66, 106–114.
- Safeeq, M., Fares, A., 2011. Accuracy evaluation of ClimGen weather generator and daily to hourly disaggregation methods in tropical conditions. *Theor. Appl. Climatol.* 106, 321–341.
- Sisman, N., Kahya, E., Aras, N., Aras, H., 2007. Determination of optimum insulation thicknesses of the external walls and roof (ceiling) for Turkey's different degree-day regions. *Energy Policy* 35, 5151–5155.
- SODA, 2014. Solar energy services for professionals. *HelioClim Solar Radiation Data, Consulting*.
- Tsilingiris, P.T., 2003. Thermal flywheel effects on time varying conduction heat transfer through structural walls. *Energy Build.* 35, 1037–1047.
- Ucar, A., Balo, F., 2009. Effect of fuel type on the optimum thickness of selected insulation materials for the four different climatic regions of Turkey. *Appl. Energy* 86, 730–736.
- Ucar, A., Balo, F., 2010. Determination of the energy savings and the optimum insulation thickness in the four different insulated exterior walls. *Renewable Energy* 35, 88–94.
- Wati, Elvis, Meukam, Pierre, Kameni Nematchoua, Modeste, Rene, Tchinda, 2015. Influence of external shading on optimum insulation thickness of building walls in a tropical region. *Appl. Therm. Eng.* 90, 754–762.
- Yu, J., Yang, C., Tian, L., Liao, D., 2009. A study on optimum insulation thicknesses of external walls in hot summer and cold winter zone of China. *Appl. Energy* 86, 2520–2529.